RESEARCH ARTICLE

Trajectory tracking anti-disturbance control for unmanned aerial helicopter based on disturbance characterization index

Linbo Chen[1] · Tao Li[1] · Lijun Liu[1] · Zehui Mao[1]

Abstract

This work studies the trajectory tracking control for unmanned aerial helicopter (UAH) system under both matched disturbance and mismatched ones. Initially, to tackle the strong coupling, an input–output feedback linearization method is utilized to simplify the nonlinear UAH system. Secondly, a set of finite-time disturbance observers (FTDOs) are proposed to estimate mismatched disturbances with their successive derivatives, which are utilized to design the feedforward controller via backstepping. Thirdly, as for matched disturbance, by defining the disturbance characterization index (DCI) to determine whether the disturbance is harmful or not for the UAH system, a feedback controller is proposed and a sufficient condition is established to ensure the convergence of the tracking error. Finally, some numerical simulations and comparisons illustrate the validity and advantages of our control scheme.

Keywords Unmanned aerial helicopter (UAH) · Trajectory tracking control · Finite-time disturbance observer (FTDO) · Backstepping control · Disturbance characterization index (DCI)

1 Introduction

In comparison with fixed-wing unmanned aircrafts, the UAHs have many advantages such as hovering, vertical take-off and landing, ultra-low-speed flight, ultra-low-altitude flight, etc., which can perform many flying missions in complex environments or narrow spaces. Then, in recent years, different scales of UAHs have been applied to practical fields including military attacks, photography, and investigation, which leads to the increasing demands for the UAHs. Yet, it is worth noting that owing to the characteristics of the UAHs, they are always sensitive to outside disturbances, which may lead to poor control performance or even aircraft crash. Therefore, it is significant to improve the anti-disturbance capability for the UAHs.

✉ Tao Li
autolitao@nuaa.edu.cn

1   College of Automation Engineering, Nanjing University of Aeronautics and Astronautics, Nanjing 211106, Jiangsu, China

Currently, as for different UAHs, most existent control schemes were mainly established based on linear UAH systems or nonlinear ones. As for linear UAH systems, these proposed techniques include PID control [1,2], LQR control [3], and H$_\infty$ control [4,5], in which the controllers were mainly designed based on the approximate linearization of nonlinear UAH systems. Yet, when the system state deviates from the set operating point, the linearized model cannot describe the accurate form and the control algorithms in [1–5] are not available, which might degrade control performance or even induce instability. Recently, some methods have been proposed to design the controllers for nonlinear UAH systems [6–13]. For instance, in [6–10], some prescribed performance-based robust adaptive nonlinear control schemes were developed for the UAH systems subject to output constraints. In [11–13], some sliding mode controllers were presented to tackle the position control for nonlinear UAH systems, in which parameter uncertainties and external disturbances were involved. Then, in this work, the nonlinear UAH system will be utilized to accomplish the controller design, which may exhibit theoretic and practical meanings.

In recent years, the feedback linearization method has been utilized to simplify the nonlinear systems [14–17]. Especially, owing to the coupling effects between transla-

tional dynamics and rotational dynamics, the UAH system always produces the unstable zero-dynamic subsystems. Then, it is always required to transform the UAH dynamic model into a minimum phase system by ignoring the body force. In [16,17], by selecting the positions and yaw angle as system outputs, an approximate feedback linearization was utilized to simplify the UAH system. In [18], the feedback linearization of small-scale UAH system was proposed, and a tracking controller for position and yaw angle was designed. By comparing with traditional control, the feedback linearization does not depend on the solution or stability of the addressed system. On the other hand, in 1990s, the backstepping control was proposed to tackle the nonlinear control systems [19]. Then, as for the UAH systems, in [20], a backstepping controller based nonlinear model was proposed to complete the automatic hovering and maneuvering flight. In [21], a flight controller based an integral backstepping control was designed for the small-scale UAH. Especially, in [22–25], the combinations of the backstepping technique and performance function-based error transformation were employed to achieve the bounded transience and steady-state tracking errors. Yet, based on the above-mentioned literature, it worth noting that although the combination of the feedback linearization and backstepping control can facilitate the controller design, it still has not been utilized to investigate the tracking control for nonlinear UAH system, which constitutes the focus of this presented work.

Meanwhile, the UAHs might be unavoidably affected by outside disturbances such as the winds and modelling error. In recent years, the anti-disturbance control has become a heated topic in the control community and a large number of results have been reported [26–28]. Based on these existing methods, the disturbance observer-based control (DOBC) has been verified to be effective in tackling the disturbed UAH systems [29–34]. Normally, according to channel and mechanism, the disturbances are divided into matched disturbance and mismatched one. For matched disturbance, its estimation can be directly incorporated into the compound control strategy, that is to say, the controller design includes both feedback control and feedforward one [28,29]. In [28], by designing the disturbance observer, the anti-saturation control for nonlinear systems was studied and the matched disturbance could be compensated directly. Yet, the model perturbation and unmodeled dynamics in a UMH system can be regarded as mismatched disturbance since they are difficult to be completely suppressed via a control channel. For instance, [30,31] utilized an improved DOBC method to suppress mismatched disturbances, and [32,33] exploited the fixed-time sliding mode DOBC to tackle the hover operations of the UAHs. It is worth noting that most DOBC methods rejected the disturbances thorough output channels using the compensation, which means that the disturbances need to be eliminated by the input signal. Yet, in some cases, the

disturbances can possess some positive effects on control performance [34]. Then, the influence of the disturbance needs to be redefined by using the disturbance characterization index (DCI), which can decide whether to retain the disturbances or not in controller design. Yet, to our best knowledge, few works have utilized the DCI concept to study the anti-disturbance control for the UAH systems, which remains important and challenging.

Motivated by the above discussions, this work will study the tracking control for the UAH system and a DCI-based anti-disturbance backstepping controller will be proposed, in which both matched disturbance and mismatched one are involved. The contributions of this work can be expressed as follows:

1. Based on the approximated feedback linearization and dynamic expansion technology, the nonlinear UAH system is simplified as an integral chain one. By combining the FTDOs and backstepping control, the virtual intermediate variables and control input are derived. Since the disturbances with successive derivatives are estimated, the repeated steps for calculating disturbance derivatives in the backstepping controller can be avoided, which can help reduce the complexity of controller design procedure.

2. Different from some existent methods that wholly eliminated the disturbances, an effective disturbance DCI-based backstepping controller scheme is developed for the UAH system under both matched disturbance and mismatched ones. For mismatched disturbance, it can be directly compensated in the backstepping controller. Yet, as for matched disturbances, a DCI definition is introduced and can determine whether the disturbance is harmful or not to the UAH system. Then, the harmful part is eliminated while the beneficial one is retained in the feedback controller, which can effectively improve the control performance.

Notations $\mathbb{R}^n$ denotes the set of n-dimensional Euclidean space, and $\mathbb{R}^{m \times n}$ means the set of all real $m \times n$ matrices. $e_3 = [0 \ 0 \ 1]^{\mathrm{T}}$ means a unitary vector. C_θ, S_θ, T_θ denote the abbreviations of trigonometric functions $\cos\theta$, $\sin\theta$, $\tan\theta$, respectively, and others are similarly abbreviated. $|x|$ stands for the absolute value for each element of the vector x. The symbol $\otimes$ represents the element-wise product.

1.1 Nonlinear dynamic model of unmanned aerial helicopter (UAH)

This subsection presents a nonlinear dynamic model for the UAH. The UAH system can be considered as a six-degree-of-freedom rigid body model with the simplified force and moment generation process, which further includes

the disturbances and parameter uncertainties as the lumped disturbances. Then, this work focuses on the full-degree-of-freedom UAH system and studies the tracking control for the position and yaw angle under outside disturbances.

Based on [15], we consider the UAH attitude dynamic system as

$$
\begin{cases}
\dot{P}(t) = V(t), \\
\dot{V}(t) = ge_3 + R(t)e_3[-g + Z_\omega \omega(t) + Z_{\text{col}}\delta_{\text{col}}(t)] \\
\qquad + d_1(t), \\
\dot{\Theta}(t) = H(\Theta)W(t), \\
\dot{W}(t) = -JW(t)^\times JW(t) + AW(t) + Bu(t) \\
\qquad + d_2(t),
\end{cases}
\tag{1}
$$

where $P(t) = [x(t)\ y(t)\ z(t)]^T \in \mathbb{R}^3$ and $V(t) = [u(t)\ v(t)\ w(t)]^T \in \mathbb{R}^3$ are the position vector and velocity vector in the inertial coordinate system, respectively; $\Theta(t) = [\phi(t)\ \vartheta(t)\ \psi(t)]^T \in \mathbb{R}^3$ and $W(t) = [p(t)\ q(t)\ r(t)]^T \in \mathbb{R}^3$ are the Euler angle vector and angular rate vector in the body-fixed frame, respectively; $\phi(t), \vartheta(t),$ and $\psi(t)$ denote the roll, pitch, and yaw angles, respectively; $p(t), q(t),$ and $r(t)$ mean the angular rates; $u(t) = [\delta_{\text{col}}(t)\ \delta_{\text{lon}}(t)\ \delta_{\text{lat}}(t)\ \delta_{\text{ped}}(t)]^T \in \mathbb{R}^4$ indicates the control input vector. The notations of $d_1(t), d_2(t)$ are the lumped disturbance vectors, which contain the wind gusts, modeling error, and uncertainties. Moreover, the notation of g denotes the gravitational acceleration, and $J = \text{diag}\{J_{xx}, J_{yy}, J_{zz}\}$ means the inertia matrix; Z_ω and Z_{col} are the stability derivative and input derivative of the main rotor thrust $T_m(t) = m[-g + Z_\omega \omega(t) + Z_{\text{col}}\delta_{\text{col}}(t)]$, respectively; $A \in \mathbb{R}^{3\times3}$ and $B \in \mathbb{R}^{3\times4}$ are the stability derivative matrix and input derivative matrix of the moment vector $\tau(t) = AW(t) + Bu(t)$, respectively. The transformation matrix $R(t) \in \mathbb{R}^3$ from the body coordinate system to the inertial coordinate one can be described as follows:

$$
R(t) = \begin{bmatrix}
C_\theta C_\psi & S_\theta C_\psi S_\phi - S_\psi C_\phi & S_\theta C_\psi C_\phi + S_\psi S_\phi \\
C_\theta S_\psi & S_\theta S_\psi S_\phi + C_\psi C_\phi & S_\theta S_\psi C_\phi - C_\psi S_\phi \\
-S_\theta & C_\theta S_\phi & C_\theta C_\phi
\end{bmatrix}.
\tag{2}
$$

The attitude Kinematirc matrix $H(\Theta)$ in system (1) is defined as

$$
H(\Theta) = \begin{bmatrix}
1 & S_\phi T_\theta & C_\phi T_\theta \\
0 & C_\phi & -S_\phi \\
0 & \dfrac{S_\phi}{C_\theta} & \dfrac{C_\phi}{C_\theta}
\end{bmatrix},
\tag{3}
$$

and the derivative of $R(t)$ is presented as

$$
\dot{R}(t) = R(t)W^\times(t),
\tag{4}
$$

where $W^\times(t) = \begin{bmatrix} 0 & -r & q \\ r & 0 & -p \\ -q & p & 0 \end{bmatrix}$.

1.2 Approximate feedback linearization model of UAH system

This subsection will utilize the input and output feedback linearization to simplify the system (1) for facilitating the controller design. Since the tracking target aims to make the UAH track the desired position $P_d(t) = [x_d(t)\ y_d(t)\ z_d(t)]^T$ and yaw angle $\psi_d(t)$, the control output can be selected as $P_d(t)$ and $\psi_d(t)$. However, the exact input–output linearization fails to linearize the complete system. Then in this work, an approximate feedback linearization technique will be developed for the UAH system [15].

It can be verified that the limped disturbances $d_1(t), d_2(t)$ are the inherent components of the UAH system, which are independent of the control input. Then, to determine the relative order, we consider the system (1) without the disturbances, i.e., the lumped disturbances need to be set as $d_1(t) = d_2(t) = 0$. Moreover, to complete the feedback linearization procedure succinctly, the term $-m[-g + Z_\omega\omega(t) + Z_{\text{col}}\delta_{\text{col}}(t)]$ should be replaced by the main rotor thrust $T_m(t)$. For completing the linearization process of UAH input and output feedback, we define two variables as $T_{1m}(t) = \dot{T}_m(t), T_{2m}(t) = \dot{T}_{1m}(t)$. Then, according to [15], the simplified model of UAH system (1) can be rewritten as

$$
\begin{cases}
\dot{P}(t) = V(t), \\
\dot{V}(t) = ge_3 - \dfrac{1}{m}R(t)e_3 T_m(t), \\
\dot{\Theta}(t) = H(\Theta)W(t), \\
\dot{W}(t) = -J^{-1}W(t)^\times JW(t) + J^{-1}\tau(t), \\
\dot{T}_m(t) = T_{1m}(t), \\
\dot{T}_{1m}(t) = T_{2m}(t).
\end{cases}
\tag{5}
$$

Here, we define $\tilde{u}(t) = [\tilde{\tau}_\phi(t)\ \tilde{\tau}_\theta(t)\ \tilde{\tau}_\psi(t)\ \tilde{T}_m(t)]^T$ as the new control input, and $\dot{W}(t) = \tilde{\tau}(t) = [\tilde{\tau}_\phi(t)\ \tilde{\tau}_\theta(t)\ \tilde{\tau}_\psi(t)]^T$. The transformation of the control signal is expressed as follows:

$$
\tilde{\tau}(t) = -J^{-1}W^\times(t)JW(t) + \tau(t).
\tag{6}
$$

To utilize the input–output feedback linearization, one can differentiate the output variables $P(t)$ and $\psi(t)$ in (5). Moreover, by defining $\zeta_1(t) = P(t), \zeta_2(t) = \dot{P}(t), \zeta_3(t) = \ddot{P}(t),$ and $\zeta_4(t) = P^{(3)}(t)$, it follows from (5) that

$$
\dot{\zeta}_1(t) = V(t),
$$

$$
\dot{\zeta}_2(t) = ge_3 - \dfrac{1}{m}R(t)e_3 T_m(t),
$$

$$\dot{\zeta}_3(t) = -\frac{1}{m}R(t)W^{\times}(t)e_3 T_m(t) - \frac{1}{m}R(t)e_3\dot{T}_m(t),$$

$$\dot{\zeta}_4(t) = f_p(t) - \frac{1}{m}R(t)K(T_m)\tau_1(t), \tag{7}$$

where $f_p(t) = -\frac{1}{m}R(t)W^{\times}(t)W^{\times}(t)e_3 T_m(t) - \frac{2}{m}\times R(t)$ $W^{\times}(t)e_3\dot{T}_m(t)$, $\tau_1(t) = [\tilde{\tau}_{\phi}(t) \ \tilde{\tau}_{\theta}(t) \ \tilde{T}_m(t)]^{\mathrm{T}}$, and

$$K(T_m) = \begin{bmatrix} 0 & T_m & 0 \\ -T_m & 0 & 0 \\ 0 & 0 & 1 \end{bmatrix}. \tag{8}$$

Now, by defining $\zeta_5(t) = \psi(t)$ and $\zeta_6(t) = \dot{\psi}(t)$, we further obtain

$$\begin{cases} \dot{\zeta}_5(t) = \psi(t), \\ \dot{\zeta}_6(t) = f_{\psi}(t) + \dfrac{S_{\phi}(t)}{C_{\theta}(t)}\tilde{\tau}_{\theta}(t) + \dfrac{C_{\phi}(t)}{C_{\theta}(t)}\tilde{\tau}_{\psi}(t), \end{cases} \tag{9}$$

where $f_{\psi}(t) = [\frac{C_{\phi}(t)}{C_{\theta}(t)}\dot{\phi}(t) + \frac{S_{\phi}(t)T_{\theta}(t)}{C_{\theta}(t)}\dot{\theta}(t)]q(t) - [\frac{S_{\phi}(t)}{C_{\theta}(t)}$ $\times\dot{\phi}(t) - \frac{C_{\phi}(t)T_{\theta}(t)}{C_{\theta}(t)}\dot{\theta}(t)]r(t)$.

Based on the above discussions, the dimension of the UAH system (1) amounts to $n = 12$, and the total relative degree is $r = 8$, which means that there must exist internal dynamics characterized via 4-D zero dynamics. Especially, by combining (7) and (9), we can obtain the relative order as $R_t = 14$. Since the dimensionality of the system (5) is $R_n = 14$, i.e., $R_t = R_n$, it can be concluded that there exists no internal dynamics in the system (1). Then, as a conclusion, the system (1) can be wholly feedback linearized.

Now, by considering the disturbances, we can obtain the complete model of the UAH system as follows:

$$S_1: \begin{cases} \dot{\zeta}_1(t) = \zeta_2(t), \\ \dot{\zeta}_2(t) = \zeta_3(t) + d_1(t), \\ \dot{\zeta}_3(t) = \zeta_4(t), \\ \dot{\zeta}_4(t) = f_p(t) - \dfrac{1}{m}R(t)K(T_m)\tau_1(t) + d_2(t), \end{cases} \tag{10}$$

$$S_2: \begin{cases} \dot{\zeta}_5(t) = \zeta_6(t), \\ \dot{\zeta}_6(t) = f_{\psi}(t) + \dfrac{S_{\phi}}{C_{\theta}}\tilde{\tau}_{\theta}(t) + \dfrac{C_{\phi}}{C_{\theta}}\tilde{\tau}_{\psi}(t) + d_3(t), \end{cases} \tag{11}$$

where $d_1(t) = [d_{11}(t) \ d_{12}(t) \ d_{13}(t)]^{\mathrm{T}} \in \mathbb{R}^3$, $d_2(t) = [d_{21}(t) \ d_{22}(t) \ d_{23}(t)]^{\mathrm{T}} \in \mathbb{R}^3$, and $d_3(t) \in \mathbb{R}$ represent the lumped disturbances. Especially, since $d_2(t)$ and $d_3(t)$ enter the helicopter system via the same channels together with the control inputs, they can be treated as the matched disturbance. However, $d_1(t)$ does not satisfy the matching condition, and it can be called mismatched disturbance. Then, as for the position and yaw angle, we define their tracking errors and

successive derivatives as

$$\begin{cases} x_n(t) = \zeta_n(t) - P_r^{(n-1)}(t), & n = 1, 2, 3, 4, \\ x_n(t) = \zeta_n(t) - \psi_r^{(n-5)}(t), & n = 5, 6, \end{cases} \tag{12}$$

where $P_r^{(n-1)}(t)$ and $\psi_r^{(n-1)}(t)$ denote the successive derivatives. Then, the tracking error system satisfies

$$\begin{cases} \dot{x}_1(t) = x_2(t), \\ \dot{x}_2(t) = x_3(t) + d_1(t), \\ \dot{x}_3(t) = x_4(t), \\ \dot{x}_4(t) = f_p(t) - \dfrac{1}{m}R(t)K(T_m)u_1(t) \\ \qquad\quad - P_r^{(4)}(t) + d_2(t), \\ \dot{x}_5(t) = x_6(t), \\ \dot{x}_6(t) = f_{\psi}(t) + \dfrac{S_{\phi}}{C_{\theta}}\tilde{\tau}_{\theta}(t) + \dfrac{C_{\psi}}{C_{\theta}}\tilde{\tau}_{\psi}(t) \\ \qquad\quad - \psi_r^{(2)}(t) + d_3(t). \end{cases} \tag{13}$$

Remark 1 It can be checked that the disturbances $d_1(t)$, $d_2(t), d_3(t)$ exist in $x_2(t)$, $x_4(t)$, and $x_6(t)$, respectively. Then, we will combine the FTDO and backstepping control to tackle mismatched disturbance $d_1(t)$, and the matched ones $d_2(t), d_3(t)$ will be rejected via the DCI-based DOBC method.

2 Finite-time disturbance observer (FTDO)

First of all, a set of FTDOs are presented to estimate the disturbances with their successive derivatives in finite time. In order to develop the subsequent FTDOs, an assumption needs to be presented.

Assumption 1 The UAH model can be described as (13), where the mismatched disturbance $d_1(t)$ satisfies at least 3-th order differentiability, and $d_1^{(4)}(t)$ possesses the Lipschitz constant L_1. The matched disturbances $d_2(t), d_3(t)$ have at least 1-st order differentiability and their first derivatives $\dot{d}_i(t)$ ($i = 2, 3$) have the Lipschitz constants L_2, L_3, respectively.

Now, a third-order FTDO is developed to estimate the disturbance $d_1(t)$ with its successive derivatives $d^{(l)}(t)$ ($l = 1, 2, 3$), which can be expressed as

$$\dot{z}_0^1(t) = \epsilon_0^1(t) + x_3(t), \tag{14}$$

$$\epsilon_0^1(t) = -\lambda_0^1 L_1^{\frac{1}{4}}|z_0^1(t) - x_2(t)|^{\frac{3}{4}}\mathrm{sgn}(z_0^1(t) - x_2(t)) + z_1^1(t), \tag{15}$$

$$\dot{z}_1^1(t) = \epsilon_1^1(t), \tag{16}$$

$$\epsilon_1^1(t) = -\lambda_1^1 L_1^{\frac{1}{3}} |z_1^1(t) - \epsilon_0^1(t)|^{\frac{2}{3}} \mathrm{sgn}(z_1^1(t) - \epsilon_0^1(t)) \\ + z_2^1(t), \tag{17}$$

$$\dot{z}_2^1(t) = \epsilon_2^1(t), \tag{18}$$

$$\epsilon_2^1(t) = -\lambda_2^1 L_1^{\frac{1}{2}} |z_2^1(t) - \epsilon_1^1(t)|^{\frac{1}{2}} \mathrm{sgn}(z_2^1(t) - \epsilon_1^1(t)) \\ + z_3^1(t), \tag{19}$$

$$\dot{z}_3^1(t) = \epsilon_3^1(t), \tag{20}$$

$$\epsilon_3^1(t) = -\lambda_3^1 L_1 \mathrm{sgn}(z_3^1(t) - \epsilon_2^1(t)), \tag{21}$$

where $z_0^1(t)$ denotes the estimate of the state $x_2(t)$; $z_1^1(t)$, $z_2^1(t)$, $z_3^1(t)$ are the estimates of the disturbance $d_1(t)$, $d_1^{(1)}(t)$, $d_1^{(2)}(t)$, respectively. Here, $L_1 > 0$ and $\lambda_i^1 > 0$ ($i = 0, 1, 2, 3$) denote the coefficients of the FTDO. In what follows, two first-order FTDOs are respectively proposed to estimate $d_2(t)$, $d_3(t)$

$$\dot{z}_0^2(t) = \epsilon_0^2(t) + f_p(t) - \frac{1}{m} R(t) K(T_m) u_1(t), \tag{22}$$

$$\epsilon_0^2(t) = -\lambda_0^2 L_2^{\frac{1}{2}} |z_0^2(t) - x_4(t)|^{\frac{1}{2}} \mathrm{sgn}(z_0^2(t) - x_4(t)) \\ + z_1^2(t), \tag{23}$$

$$\dot{z}_1^2(t) = \epsilon_1^2(t), \tag{24}$$

$$\epsilon_1^2(t) = -\lambda_1^2 L_2 \mathrm{sgn}(z_1^2(t) - \epsilon_0^2(t)), \tag{25}$$

$$\dot{z}_0^3(t) = \epsilon_0^3(t) + f_\psi(t) + \frac{S_\phi}{C_\theta} \tilde{\tau}_\theta(t) + \frac{C_\psi}{C_\theta} \tilde{\tau}_\psi(t), \tag{26}$$

$$\epsilon_0^3(t) = -\lambda_0^3 L_3^{\frac{1}{2}} |z_0^3(t) - x_6(t)|^{\frac{1}{2}} \mathrm{sgn}(z_0^3(t) - x_6(t)) \\ + z_1^3(t), \tag{27}$$

$$\dot{z}_1^3(t) = \epsilon_1^3(t), \tag{28}$$

$$\epsilon_1^3(t) = -\lambda_1^3 L_3 \mathrm{sgn}(z_1^3(t) - \epsilon_0^3(t)), \tag{29}$$

where $z_0^i(t)$ ($i = 2, 3$) denote the estimates of the states $x_j(t)$ ($j = 4, 6$), and $z_1^i(t)$ ($i = 2, 3$) mean the estimates of the disturbances $d_i(t)$ ($i = 2, 3$). Moreover, $L_j > 0$ ($j = 2, 3$) and $\lambda_i^j > 0$ ($i = 0, 1; j = 2, 3$) mean the coefficients of the proposed FTDOs.

Considering the tracking error system (13), the error dynamics of the FTDO (14) described in the Filippov sense can be presented as

$$\begin{cases} \dot{e}_0^1(t) = -\lambda_0^1 L_1^{\frac{1}{4}} |e_0^1(t)|^{\frac{3}{4}} \mathrm{sgn}(e_1^0) + e_1^1(t), \\ \dot{e}_1^1(t) = -\lambda_1^1 L_1^{\frac{1}{3}} |e_1^1(t) - \dot{e}_0^1(t)|^{\frac{2}{3}} \mathrm{sgn}(e_1^1(t) - \dot{e}_1^0(t)) \\ \qquad + e_2^1(t), \\ \dot{e}_2^1(t) = -\lambda_2^1 L_1^{\frac{1}{2}} |e_2^1(t) - \dot{e}_1^1(t)|^{\frac{1}{2}} \mathrm{sgn}(e_2^1(t) - \dot{e}_1^1(t)) \\ \qquad + e_3^1(t), \\ \dot{e}_3^1(t) = -\lambda_3^1 L_1 \mathrm{sgn}(e_3^1(t) - \dot{e}_2^1(t)) + [-L_1, L_1], \end{cases} \tag{30}$$

where the FTDO estimate errors are defined as $e_0^1(t) = z_0^1(t) - x_2(t)$, $e_1^1(t) = z_1^1(t) - d_1(t)$, $e_2^1(t) = z_2^1(t) - d_1^{(1)}(t)$, and $e_3^1(t) = z_3^1(t) - d_1^{(2)}(t)$. It follows from [15] that the estimate errors $e_i^1(t)$ ($i = 0, 1, 2, 3$) will converge to be convergent in finite time, which implies that there must exist a time second t_f such that $e_i^1(t) = 0$ for any $t > t_f$. That is to say, $z_i^1(t) = \epsilon_{i-1}^1(t)$ ($i = 1, 2, 3$) hold for any $t > t_f$. Similarly, we can derive the error dynamics of the FTDOs for (22) and (26) as follows:

$$\begin{cases} \dot{e}_0^2(t) = -\lambda_0^2 L_2^{\frac{1}{2}} |e_0^2(t)|^{\frac{1}{2}} \mathrm{sgn}(e_0^2) + e_1^2(t), \\ \dot{e}_1^2(t) = -\lambda_1^2 L_2 \mathrm{sgn}(e_1^2(t) - \dot{e}_1^2(t)) + [-L_2, L_2], \end{cases} \tag{31}$$

$$\begin{cases} \dot{e}_0^3(t) = -\lambda_0^3 L_3^{\frac{1}{2}} |e_0^3(t)|^{\frac{1}{2}} \mathrm{sgn}(e_0^3) + e_1^3(t), \\ \dot{e}_1^3(t) = -\lambda_1^3 L_3 \mathrm{sgn}(e_1^3(t) - \dot{e}_1^3(t)) + [-L_3, L_3]. \end{cases} \tag{32}$$

Based on [15], the stability of the error systems (31)–(32) can be guaranteed in finite time, which also implies that there must exist a time second t_f such that $e_i^j(t) = 0$ ($i = 2, 3; j = 0, 1$) for any $t > t_f$.

3 Tracking controller design

In this section, a DCI-based DOBC and backstepping control method will be presented to tackle the tracking control for the UAH system under external disturbances.

3.1 Backstepping controller

Defining the tracking variables $\eta_1(t)$ and $\eta_2(t)$ as

$$\eta_1(t) = x_1(t) - x_{1d}(t), \ \eta_2(t) = x_2(t) - x_{2d}(t), \tag{33}$$

where $x_{1d}(t)$, $x_{2d}(t)$ are the virtual control variables, they can be further designed as follows:

$$x_{1d}(t) = 0, \ x_{2d}(t) = -k_1 \eta_1(t). \tag{34}$$

Then, the Lyapunov function of $\eta_1(t)$ with its derivative can be derived as

$$\begin{cases} V_1(t) = \frac{1}{2} \eta_1^T(t) \eta_1(t), \\ \dot{V}_1(t) = \eta_1^T(t)[-k_1 \eta_1(t) + \eta_2(t)], \end{cases} \tag{35}$$

where k_1 denotes the controller parameter. Moreover, the Lyapunov function of $\eta_2(t)$ with its derivative can be deduced as

$$\begin{cases} V_2(t) = \frac{1}{2} \eta_2^T(t) \eta_2(t), \\ \dot{V}_2(t) = \eta_2^T(t)[x_3(t) + d_1(t) - \dot{x}_{2d}(t)]. \end{cases} \tag{36}$$

Define $\eta_3(t) = x_3(t) - x_{3d}(t)$ with $x_{3d}(t)$ being expressed as

$$x_{3d}(t) = -k_2\eta_2(t) + \dot{x}_{2d}(t) - z_1^1(t). \tag{37}$$

Here, $x_{3d}(t)$ can compensate for the disturbance $d_1(t)$, and k_2 denotes the controller parameter. Moreover, $\dot{V}_2(t)$ can be rewritten as

$$\dot{V}_2(t) = \eta_2^{\mathrm{T}}(t)[-k_2\eta_2(t) + \eta_3(t)]. \tag{38}$$

Then, the Lyapunov function of $\eta_3(t)$ and its derivative can be obtained as

$$\begin{cases} V_3(t) = \dfrac{1}{2}\eta_3^{\mathrm{T}}(t)\eta_3(t), \\ \dot{V}_3(t) = \eta_3^{\mathrm{T}}(t)\dot{\eta}_3(t) = \eta_3^{\mathrm{T}}(t)[x_4(t) - \dot{x}_{3d}(t)]. \end{cases} \tag{39}$$

Now, we define $\eta_4(t) = x_4(t) - x_{4d}(t)$, and $x_{4d}(t)$ is expressed as

$$x_{4d}(t) = -k_3\eta_3(t) + \dot{x}_{3d}(t), \tag{40}$$

where k_3 means the controller parameter. Then, $\dot{V}_3(t)$ can be written as

$$\begin{aligned} \dot{V}_3(t) &= \eta_3^{\mathrm{T}}(t)[\eta_4(t) + x_{4d}(t) - \dot{x}_{3d}(t)] \\ &= \eta_3^{\mathrm{T}}(t)[-k_3\eta_3(t) + \eta_4(t)]. \end{aligned} \tag{41}$$

The Lyapunov function of $\eta_4(t)$ with its derivative can be obtained as $V_4(t) = \frac{1}{2}\eta_4^{\mathrm{T}}(t)\eta_4(t)$, and

$$\begin{aligned} \dot{V}_4(t) &= \eta_4^{\mathrm{T}}(t)[f_p(t) - \frac{1}{m}R(t)K(T_m)u_1(t) \\ &\quad - P_r^{(4)}(t) + d_2(t) - \dot{x}_{4d}(t)]. \end{aligned} \tag{42}$$

Now, the control law $u_1(t)$ can be designed as

$$\begin{aligned} u_1(t) &= mK^{-1}(T_m)R^{\mathrm{T}}(t)[f_p(t) - P_r^{(4)}(t) \\ &\quad + \dot{x}_{4d}(t) + k_4\eta_4(t)]. \end{aligned} \tag{43}$$

Therefore, it follows from (42) and (43) that

$$\dot{V}_4(t) = -k_4\eta_4^{\mathrm{T}}(t)\eta_4(t) + \eta_4^{\mathrm{T}}(t)d_2(t), \tag{44}$$

where k_4 denotes the controller parameter.

On the other hand, by defining the tracking variable $\eta_5(t) = x_5(t) - x_{5d}(t)$, then the virtual control variable $x_{5d}(t)$ can be designed as

$$x_{5d}(t) = 0. \tag{45}$$

The Lyapunov function of $\eta_5(t)$ with its derivative can be obtained as follows:

$$V_5(t) = \frac{1}{2}\eta_5^{\mathrm{T}}(t)\eta_5(t), \ \dot{V}_5(t) = \eta_5^{\mathrm{T}}(t)x_6(t). \tag{46}$$

Defining $\eta_6(t) = x_6(t) - x_{6d}(t)$, then $x_{6d}(t)$ can be designed as

$$x_{6d}(t) = -k_5\eta_5(t), \tag{47}$$

where k_5 is the controller parameter. Therefore, $\dot{V}_5(t)$ can be further written as

$$\begin{aligned} \dot{V}_5(t) &= \eta_5^{\mathrm{T}}(t)[x_{6d}(t) + \eta_6(t)] \\ &= \eta_5^{\mathrm{T}}(t)[-k_5\eta_5(t) + \eta_6(t)]. \end{aligned} \tag{48}$$

The Lyapunov function of $\eta_6(t)$ and its derivative can be obtained as

$$\begin{aligned} V_6(t) &= \frac{1}{2}\eta_6^{\mathrm{T}}(t)\eta_6(t), \\ \dot{V}_6(t) &= \eta_6^{\mathrm{T}}(t)[f_\psi(t) + \frac{S_\phi}{C_\theta}\tilde{\tau}_\theta(t) + \frac{C_\phi}{C_\theta}\tilde{\tau}_\psi(t) \\ &\quad - \psi_r^{(2)}(t) + d_3(t) - \dot{x}_{6d}(t)]. \end{aligned} \tag{49}$$

Thus, the control law $\tilde{\tau}_\psi(t)$ can be designed as

$$\begin{aligned} \tilde{\tau}_\psi(t) &= -\frac{C_\theta}{C_\phi}[k_6\eta_6(t) + f_\psi(t) + \frac{S_\phi}{C_\theta}\tilde{\tau}_\theta(t) \\ &\quad - \psi_r^{(2)}(t) - \dot{x}_{6d}(t)], \end{aligned} \tag{50}$$

where k_6 means the controller parameter. Therefore, it follows from (50) that

$$\dot{V}_6(t) = \eta_6^{\mathrm{T}}(t)[-k_6\eta_6(t) + d_3(t)]. \tag{51}$$

Since $d_1(t)$ is the mismatched disturbance, it can be compensated during the design of the backstepping controller. Yet, as for the matched ones $d_i(t)$ $(i = 2, 3)$, a new method based disturbance characterization index (DCI) is proposed to improve the tracking control performance, which can utilize the positive effects of the disturbances. Now, under the conventional backstepping control laws in the last section, we can select the Lyapunov function for the system (13) and compute out its time derivative as follows:

$$
\begin{cases}
V(t) = V_1(t) + V_2(t) + V_3(t) + V_4(t) + V_5(t) + V_6(t), \\
\dot{V}(t) = -k_1 \eta_1^{\mathrm{T}}(t)\eta_1(t) + \eta_1^{\mathrm{T}}(t)\eta_2(t) - k_2 \eta_2^{\mathrm{T}}(t)\eta_2(t) \\
\quad + \eta_2^{\mathrm{T}}(t)\eta_3(t) - k_3 \eta_3^{\mathrm{T}}(t)\eta_3(t) + \eta_3^{\mathrm{T}}(t)\eta_4(t) \\
\quad - k_4 \eta_4^{\mathrm{T}}(t)\eta_4(t) + \eta_4^{\mathrm{T}}(t)d_2(t) - k_5 \eta_5^{\mathrm{T}}(t)\eta_5(t) \\
\leq +\eta_5^{\mathrm{T}}(t)\eta_6(t) - k_6 \eta_6^{\mathrm{T}}(t)\eta_6(t) + \eta_6^{\mathrm{T}}(t)d_3(t) \\
\quad - \left(k_1 - \dfrac{1}{2}\right)\eta_1^{\mathrm{T}}(t)\eta_1(t) - (k_2 - 1)\eta_2^{\mathrm{T}}(t)\eta_2(t) \\
\quad - (k_3 - 1)\eta_3^{\mathrm{T}}(t)\eta_3(t) - \left(k_4 - \dfrac{1}{2}\right)\eta_4^{\mathrm{T}}(t)\eta_4(t) \\
\quad - (k_5 - \dfrac{1}{2})\eta_5^{\mathrm{T}}(t)\eta_5(t) - \left(k_6 - \dfrac{1}{2}\right)\eta_6^{\mathrm{T}}(t)\eta_6(t) \\
\quad + \eta_4^{\mathrm{T}}(t)d_2(t) + \eta_6^{\mathrm{T}}(t)d_3(t).
\end{cases}
\tag{52}
$$

Based on the term (52), by choosing the suitable scalars k_i $(i = 1, 2, \ldots, 6)$, we can acquire that $-(k_1 - \frac{1}{2})\eta_1^{\mathrm{T}}(t)\eta_1(t)$ $-(k_2 - 1)\eta_2^{\mathrm{T}}(t)\eta_2(t) - (k_3 - 1)\eta_3^{\mathrm{T}}(t)\eta_3(t) - \left(k_4 - \frac{1}{2}\right)\eta_4^{\mathrm{T}}(t)\eta_4$ $(t) - (k_5 - \frac{1}{2})\eta_5^{\mathrm{T}}(t)\eta_5(t) - \left(k_6 - \frac{1}{2}\right)\eta_6^{\mathrm{T}}(t)\eta_6(t) < 0$ holds. Then, the derivative of $V(t)$ satisfies $\dot{V}(t) < \eta_4^{\mathrm{T}}(t)d_2(t) + \eta_6^{\mathrm{T}}(t)d_3(t)$. Thus, it is worth noting whether $\dot{V}(t)$ to be negative or not depends on the term $\eta_4^{\mathrm{T}}(t)d_2(t) + \eta_6^{\mathrm{T}}(t)d_3(t)$. Especially, when $\eta_4^{\mathrm{T}}(t)d_2(t) < 0$ and $\eta_6^{\mathrm{T}}(t)d_3(t) < 0$ hold, then $\dot{V}(t) < 0$ holds and the stability of error system can be guaranteed, which shows that the disturbances $d_2(t), d_3(t)$ are beneficial for the UAH system. Yet, if $\eta_4^{\mathrm{T}}(t)d_2(t) \geq 0$ and $\eta_6^{\mathrm{T}}(t)d_3(t) \geq 0$ hold, then $\dot{V}(t) < 0$ cannot be true, which means that the disturbances $d_i(t)$ $(i = 2, 3)$ are detrimental to the UAH system. Motivated by the above discussions, we introduce a DCI definition, which indicates the beneficial or harmful effects of the disturbances acting on the UAH system. Meanwhile, since the disturbances $d_i(t)$ $(i = 2, 3)$ cannot be directly measured, the definition of the DCI will be presented by utilizing the estimations based on the FTDOs (14)–(26).

Definition 1 [34] Considering the Lyapunov functions (44) and (51), the DCI can be defined as

$$
\begin{cases}
J_{d_2} = \mathrm{sgn}(\eta_4) \otimes \mathrm{sgn}(z_1^2), \\
J_{d_3} = \mathrm{sgn}(\eta_6) \otimes \mathrm{sgn}(z_1^3).
\end{cases}
\tag{53}
$$

Remark 2 As illustrated in Definition 1, $J_{d_2} = [J_{d_{21}} \ J_{d_{22}} \ J_{d_{23}}]^{\mathrm{T}}$ denotes the 3×1 vector owing to that both η_4 and z_1^2 (estimation of d_2) are 3×1 vectors, and J_{d_3} is a variable. Then, J_{d_2} and J_{d_3} can be rewritten as

$$
\begin{cases}
J_{d_2} = [J_{d_{21}} \ J_{d_{22}} \ J_{d_{23}}]^{\mathrm{T}}, \\
J_{d_3} = \mathrm{sgn}(\eta_6)\mathrm{sgn}(z_1^3)
\end{cases}
\tag{54}
$$

with $J_{d_{2i}} = \mathrm{sgn}(\eta_{4i})\mathrm{sgn}(z_{1i}^2)$ $(i = 1, 2, 3)$.

3.2 Disturbance charaterization-based backstepping controller (DCBBC)

In this part, we will propose the design method for the disturbance charaterization-based backstepping controller (DCBBC). Based on the DCI definition, a switching control strategy will be developed for the control target of the UAH system, and the details will be described in the following theorem.

Theorem 1 *Given the scalars $k_i > \frac{1}{2}$ $(i = 1, 4, 5, 6)$, $k_j > 1$ $(j = 2, 3)$ in (38), the tracking errors $\eta_i(t)$ $(i = 1, 2, 3, 4, 5, 6)$ can asymptotically converge to zero, if the DCBBC for the UAH system (13) is designed as*

$$
\begin{cases}
u_1(t) = mK^{-1}(T_m)R^{\mathrm{T}}(t)[f_p(t) - P_r^{(4)}(t) \\
\quad + \dot{x}_{4d}(t) + k_4\eta_4(t) - \varXi(J_{d_2})z_1^2(t)], \\
\tilde{\tau}_\psi(t) = -\dfrac{C_\theta}{C_\phi}[k_6\eta_6(t) + f_\psi(t) + \dfrac{S_\phi}{C_\theta}\tilde{\tau}_\theta(t) \\
\quad - \psi_r^{(2)}(t) - \dot{x}_{6d}(t) - \varXi(J_{d_3})z_1^3(t)],
\end{cases}
\tag{55}
$$

where the DCIs, J_{d_2}, J_{d_3} are given in (54), the function $\varXi(J_{d_2})$ is expressed as $\varXi(J_{d_2}) = \mathrm{diag}\{\rho(\gamma_1) \ \rho(\gamma_2) \ \rho(\gamma_3)\}$, $\varXi(J_{d_3})$ is given as $\varXi(J_{d_3}) = \rho(\gamma_4)$, and the function $\rho(\cdot)$ is selected as

$$
\rho(\gamma_i) =
\begin{cases}
1, & \gamma_i \leq 0, \\
0, & \gamma_i < 0.
\end{cases}
\tag{56}
$$

Proof By substituting the control law (55) into the UAH system (13), we choose the Lyapunov function as the one in (52), i.e.,

$$
V(t) = \sum_{i=1}^{6} V_i(t),
\tag{57}
$$

where the terms $V_i(t)$ $(i = 1, 2, 3, 4, 5, 6)$ are separately expressed in (35), (38), (41), (44), (48), and (51). Then, we compute out and estimate its derivative as

$$
\begin{aligned}
\dot{V}(t) \leq &-\left(k_1 - \frac{1}{2}\right)\eta_1^{\mathrm{T}}(t)\eta_1(t) - (k_2 - 1)\eta_2^{\mathrm{T}}(t)\eta_2(t) \\
&- (k_3 - 1)\eta_3^{\mathrm{T}}(t)\eta_3(t) - \left(k_4 - \frac{1}{2}\right)\eta_4^{\mathrm{T}}(t)\eta_4(t) \\
&- (k_5 - \frac{1}{2})\eta_5^{\mathrm{T}}(t)\eta_5(t) - \left(k_6 - \frac{1}{2}\right)\eta_6^{\mathrm{T}}(t)\eta_6(t) \\
&+ \eta_4^{\mathrm{T}}(t)[d_2(t) - \varXi(J_{d_2})z_1^2(t)] + \eta_6^{\mathrm{T}}(t)[d_3(t) \\
&- \varXi(J_{d_3})z_1^3(t)].
\end{aligned}
\tag{58}
$$

Moreover, since $k_i > \frac{1}{2}$ ($i = 1, 4, 5, 6$) and $k_j > 1$ ($j = 2, 3$) hold, we can further deduce

$$\dot{V}(t) \le \eta_4^T(t)[d_2(t) - \Xi(J_{d_2})z_1^2(t)] \\ + \eta_6^T(t)[d_3(t) - \Xi(J_{d_3})z_1^3(t)]. \tag{59}$$

Meanwhile, since the function $\Xi(\cdot)$ is symmetric, then $\Xi(J_{d_2})$, $\Xi(J_{d_3})$ have the following expressions:

$$\begin{cases} \Xi(J_{d_2}) = \text{diag}\{\rho(\eta_{41}z_{11}^2), \rho(\eta_{42}z_{12}^2), \rho(\eta_{43}z_{13}^2)\}, \\ \Xi(J_{d_3}) = \rho(\eta_6 z_1^3). \end{cases} \tag{60}$$

Then, the item $\eta_4^T(t)[d_2(t) - \Xi(J_{d_2})z_1^2(t)]$ can be rewritten as

$$\eta_4^T(t)[d_2(t) - \Xi(J_{d_2})z_1^2(t)] \\ = \eta_4^T(t)\{[d_2(t) - z_1^2(t)] + [z_1^2(t) - \Xi(J_{d_2})z_1^2(t)]\} \\ = \eta_4^T(t)[d_2(t) - z_1^2(t)] + \eta_4^T(t)[z_1^2(t) - \Xi(J_{d_2})z_1^2(t)] \\ = \eta_4^T(t)[d_2(t) - z_1^2(t)] \\ + \sum_{i=1}^{3}[1 - \rho(\eta_{4i}z_{1i}^2)]\eta_{4i}(t)z_{1i}^2(t). \tag{61}$$

Similarly, the term $\eta_6^T(t)[d_3(t) - \Xi(J_{d_3})z_1^3(t)]$ can be also written as

$$\eta_6^T(t)[d_3(t) - \Xi(J_{d_3})z_1^3(t)] \\ = \eta_6(t)[d_3(t) - z_1^3(t)] + [1 - \rho(\eta_6 z_1^3)]\eta_6(t)z_1^3(t). \tag{62}$$

Now, by considering $[1 - \rho(\eta_{4i}z_{1i}^2)]\eta_{4i}(t)z_{1i}^2(t) < 0$ and $[1 - \rho(\eta_6 z_1^3)]\eta_6(t)z_1^3(t) < 0$, it follows from (59)–(62) that $\dot{V}(t)$ satisfies the following condition:

$$\dot{V}(t) \le \eta_4^T(t)[d_2(t) - z_1^2(t)] + \eta_6^T(t)[d_3(t) - z_1^3(t)] \\ = \eta_4^T(t)e_1^2(t) + \eta_6^T(t)e_1^3(t) \\ \le \frac{1}{2}\eta_4^T(t)\eta_4(t) + \frac{1}{2}\eta_6^T(t)\eta_6(t) \\ + \frac{1}{2}(e_1^2(t))^T e_1^2(t) + \frac{1}{2}(e_1^3(t))^T e_1^3(t) \\ \le V(t) + \frac{1}{2}(e_1^2(t))^T e_1^2(t) + \frac{1}{2}(e_1^3(t))^T e_1^3(t). \tag{63}$$

Therefore, $V(t)$ and $\eta_i(t)$ ($i = 1, 2, \ldots, 6$) will not escape to infinity in the finite time.

Next, we will show that the tracking errors $\eta_i(t)$ ($i = 1, 2, \ldots, 6$) will converge to zero in an asymptotic way. Based on the FTDOs in (14)–(26), we can obtain that the disturbance estimations $z_1^1(t)$, $z_1^2(t)$, $z_1^3(t)$ will converge to real disturbances $d_i(t)$ ($i = 1, 2, 3$) in the finite time, which illustrates that there must exist a time moment $t_f > 0$ ensuring $z_1^i(t) = d_i(t)$ ($i = 1, 2, 3$) for $t > f_f$. Therefore, as for

$t > t_f$, since $\eta_4^T(t)e_1^2(t) + \eta_6^T(t)e_1^3(t)$ is converted to zero, then it follows from (58) that

$$\dot{V}(t) \le -\left(k_1 - \frac{1}{2}\right)\eta_1^T(t)\eta_1(t) - (k_2 - 1)\eta_2^T(t)\eta_2(t) \\ - (k_3 - 1)\eta_3^T(t)\eta_3(t) \\ - \left(k_4 - \frac{1}{2}\right)\eta_4^T(t)\eta_4(t) - (k_5 - \frac{1}{2})\eta_5^T(t)\eta_5(t) \\ - \left(k_6 - \frac{1}{2}\right)\eta_6^T(t)\eta_6(t). \tag{64}$$

Moreover, by recalling $k_i > \frac{1}{2}$ ($i = 1, 4, 5, 6$) and $k_j > 1$ ($j = 2, 3$), we can further deduce

$$\dot{V}(t) < 0, \ \forall \ \eta_i(t) \ne 0 \ (i = 1, 2, \ldots, 6). \tag{65}$$

In summary, the tracking errors converge to zero asymptotically, and the proof is completed. $\qquad\square$

Remark 3 In this work, the UAH system includes both matched disturbance and mismatch one, which are separately tackled in the procedures of controller design. As for the mismatched disturbance, it is directly compensated by using the backstepping control steps (37). Yet, as for the matched one, different from these existent works [35–38], we introduce the DCI concept to decide whether the disturbances are harmful or beneficial to the UAH system. Then, by applying the DCI to estimate the derivative of Lyapunov functional, our proposed methods keep the beneficial parts but remove the harmful ones, which can help improve the control performance in an effective way.

4 Simulated example

Based on [35], we assume that the disturbances $d_i(t)$ ($i = 1, 2, 3$) are generated by the following exogenous systems:

$$\begin{cases} \dot{\zeta}_i(t) = W_i\zeta_i(t), \\ d_i(t) = V_i\zeta_i(t), \end{cases} \tag{66}$$

where $\zeta_i(t) \in \mathbb{R}^{n_{\zeta_i}}$ ($i = 1, 2, 3$) denote the states of the systems (66), and W_i, V_i are expressed as follows:

$$W_1 = \begin{bmatrix} 0 & 1.5 & 0 & 0 \\ -1.5 & 0 & 0 & 0 \\ 0 & 0 & 0 & -1 \\ 0 & 0 & 1 & 0 \end{bmatrix}, \quad W_2 = \begin{bmatrix} 0 & -2 & 0 & 0 \\ 2 & 0 & 0 & 0 \\ 0 & 0 & 0 & -1 \\ 0 & 0 & 1 & 0 \end{bmatrix},$$

$$W_3 = \begin{bmatrix} 0 & 1.5 & 0 & 0 \\ -1.5 & 0 & 0 & 0 \\ 0 & 0 & 0 & -2 \\ 0 & 0 & 2 & 0 \end{bmatrix}, \quad V_1 = \begin{bmatrix} 1 & 1 & 0.5 & -0.7 \\ 0.5 & 1 & 0 & 1 \\ 1 & 0 & 1 & 0.5 \end{bmatrix},$$
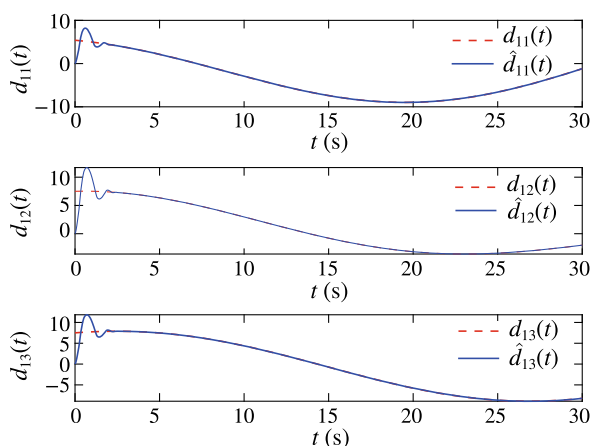
Fig. 1 The disturbances $d_1(t)$ and its estimations

Fig. 2 The disturbances $d_2(t)$ and its estimations

$$V_2 = \begin{bmatrix} 1 & 0.2 & 0 & 1 \\ -0.6 & 1 & 1 & 0 \\ 1 & 0 & 1 & 0.5 \end{bmatrix}, \quad V_3 = \begin{bmatrix} 1 & 0.2 & 0 & 1 \end{bmatrix}.$$

In what follows, firstly, some numerical simulations are provided to demonstrate the effectiveness of our FTDO-based DCBBC methods. Secondly, some comparisons with existent DOBC methods are presented to evaluate the superiorities of our control scheme.

Based on [15], the parameters of the UAH system are given as $m = 8.2\,\mathrm{kg}$, $g = 9.81\,\mathrm{m\,s^{-2}}$, $Z_w = -0.76\,\mathrm{s^{-1}}$, $Z_{\mathrm{col}} = -131.41\,\mathrm{m\,rad^{-1}\,s^{-2}}$, $J = \mathrm{diag}\{0.18, 0.34, 0.28\}\,\mathrm{kg\,m^2}$, $A = \mathrm{diag}\{-48.1757, -25.5048, -0.9080\}\,\mathrm{s^{-1}}$, and

$$B = \begin{bmatrix} 0 & 0 & 1689.5 & 0 \\ 0 & 894.5 & 0 & 0 \\ -0.3705 & 0 & 0 & 135.8 \end{bmatrix}\,\mathrm{s^{-2}}. \tag{67}$$

Moreover, the coefficients of the FTDOs in (14)–(26) are selected as $\lambda_0^1 = 4$, $\lambda_1^1 = 3$, $\lambda_2^1 = 3$, $\lambda_3^1 = 4$, $L_1 = 10$, $\lambda_0^2 = 4$, $\lambda_1^2 = 4$, $L_2 = 15$, $\lambda_0^3 = 3$, $\lambda_1^3 = 3$, $L_3 = 10$.

The control gains of the DCBBC in (55) are expressed as $k_1 = 15$, $k_2 = 18$, $k_3 = 16$, $k_4 = 18$, $k_5 = 18$, $k_6 = 10$. The desired reference trajectories of the position and yaw angle are set as follows:

$$\begin{bmatrix} u_d \\ v_d \\ w_d \end{bmatrix} = \begin{bmatrix} 0 \\ 0 \\ 1.5 \end{bmatrix} + \begin{bmatrix} 0.8\cos t \\ 0.6\sin t \\ 2\cos(0.8t) \end{bmatrix}, \quad \psi_d = 2\sin(0.5t).$$

The simulation results are shown from Figs. 1, 2, 3, 4, 5, 6, 7, 8, 9, 10 and 11. Figures 1, 2 and 3 depict the disturbance estimations by using the proposed FTDOs. It can be observed that the FTDOs can estimate the disturbances efficiently. Figures 4, 5, 6 and 7 illustrate the response curves of the position and yaw angle, respectively, which means that the reference trajectories can be tracked accurately under our
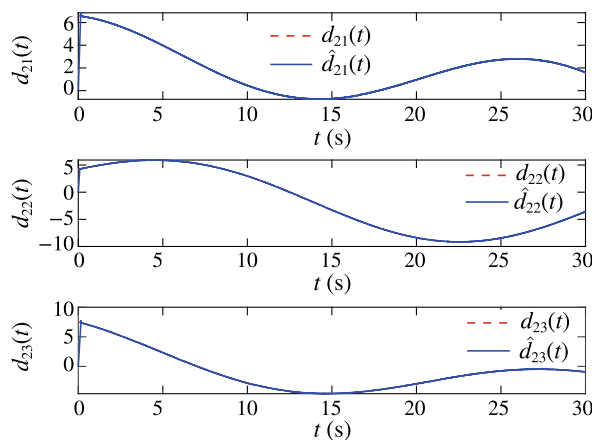

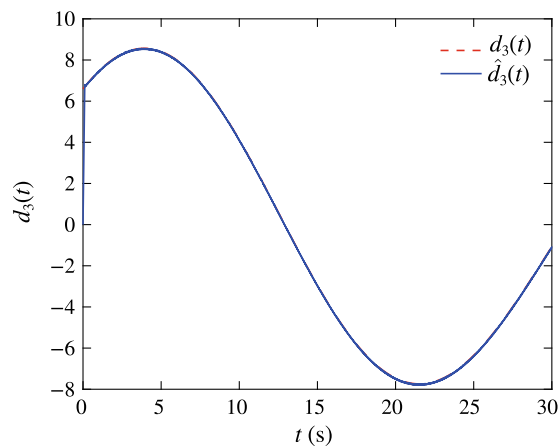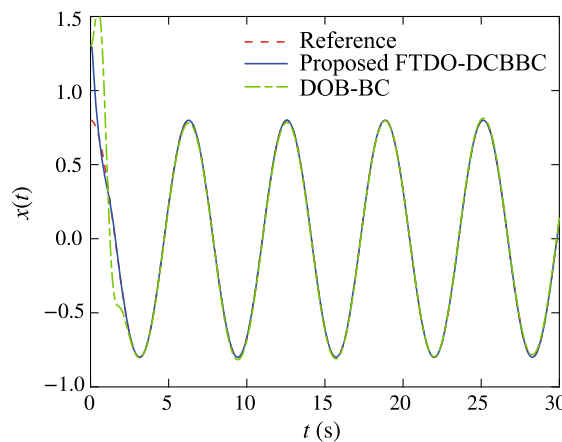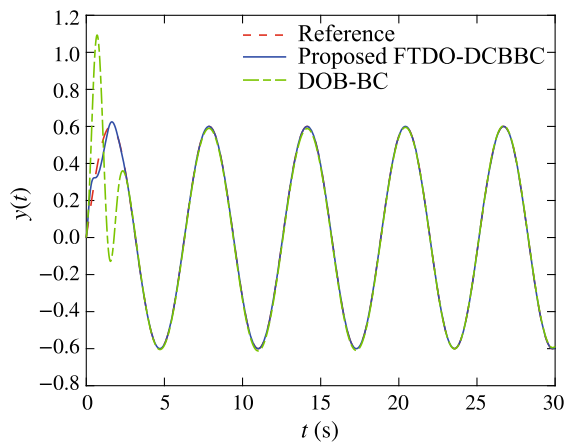Fig. 3 The disturbances $d_3(t)$ and its estimations

Fig. 4 The response curves of the position $x(t)$

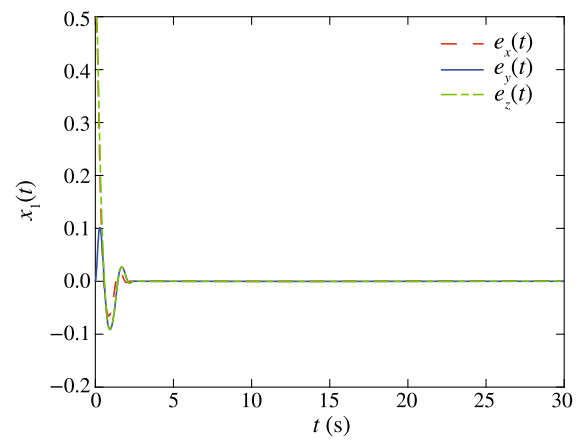**Fig. 5** The response curves of the position $y(t)$

Fig. 6 The response curves of the position $z(t)$
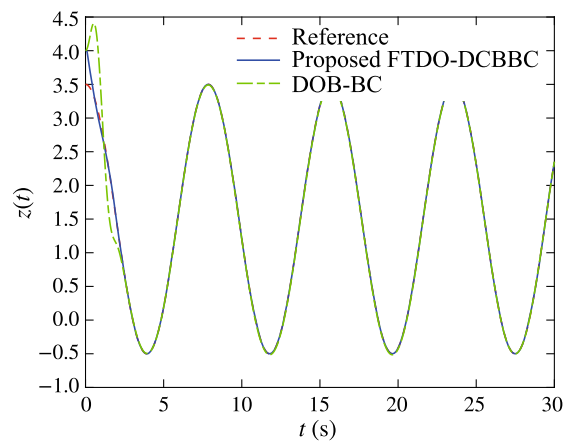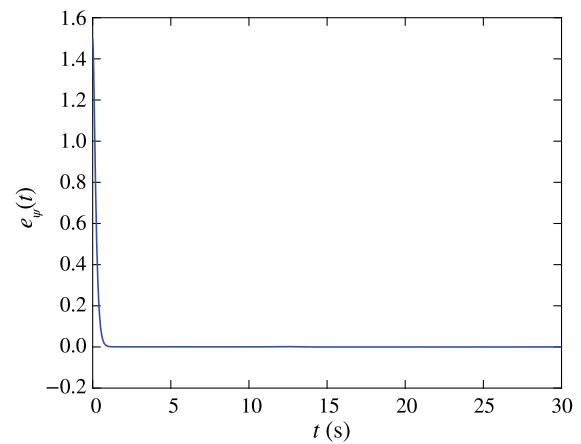

Fig. 7 The response curves of the yaw angle $\psi(t)$

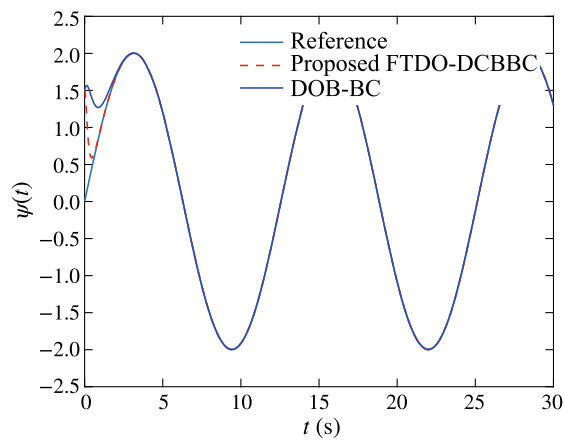**Fig. 8** The response curves of the position tracking error

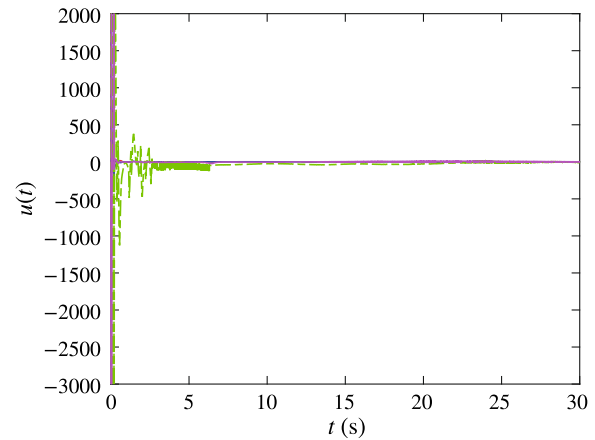**Fig. 9** The response curves of the yaw angle $\psi(t)$ tracking error

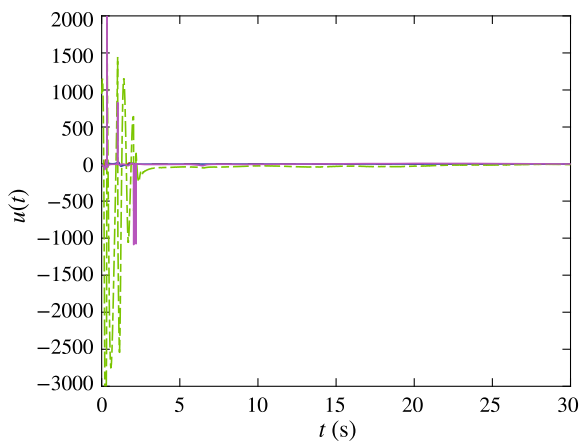**Fig. 10** The response curves of the control under the proposed FTDO-DCBBC method

Fig. 11 The response curves of the control under the DOBC method

Table 1 The RMS values of the tracking errors

Methods	FTDO-DCBBC	DOBC
$(e_x)_{\text{RMS}}$	0.0002155	0.01332
$(e_y)_{\text{RMS}}$	0.00007969	0.006545
$(e_z)_{\text{RMS}}$	0.00005112	0.005398
$(e_\psi)_{\text{RMS}}$	0.003278	0.005713

proposed FTDO-DCBBC methods. Especially, the FTDO-DCBBC method in this work can be superior over some traditional DOBC ones. From Figs. 4, 5, 6 and 7, it can be seen that the overshoots by our FTDO-DCBBC method are smaller than the one by the DOBC method in some degree. Figures 8 and 9 show the tracking errors of the position and yaw angle, from which the tracking errors can converge to zero in a finite time.

Now, based on the tradition backstepping controller, we choose the similar parameters and further present some comparisons [35], which can be checked in Figs. 10 and 11. Then, based on the response curves of the control laws in Figs. 10 and 11, we can check that the control performance by our method is better than the one by the DOBC method since the trajectories fluctuates is much smaller in the early time interval. Moreover, to highlight the merits of our method, the root-mean-square (RMS) values of the tracking errors under the FTDO-DCBBC method and the DOBC are summarized in Table 1. As illustrated in Table 1, the proposed FTDO-DCBBC method achieves lower RMS values than the traditional DOBC, which reveals that our method can be superior over the existent ones.

5 Conclusions

In this work, the trajectory tracking control for the UAH system under both matched disturbance and mismatched ones has been investigated. First, the input–output feedback linearization method was utilized to simplify the nonlinear UAH system, which could avoid the strong coupling. Then, some effective FTDOs were presented to estimate the disturbances with their successive derivatives. Thirdly, based on the backstepping control and proposed FTDOs, a tracking control scheme was offered and it could compensate for the mismatched disturbance directly. Moreover, by utilizing the DCI concept, an anti-disturbance backstepping controller was presented, and it could contain the beneficial effects of the matched disturbances, which might lead to better control performance. Finally, some simulations and comparisons have been exploited to demonstrate the effectiveness of the proposed control methods.

References

1. Garcia, R. A., Rubio, F. R., & Ortega, M. G. (2012). Robust PID control of the quadrotor helicopter. *IFAC Proceedings Volumes, 45*(3), 229–234.
2. Fang, X., Liu, F., & Zhao, S. Y. (2007). Combining fuzzy, PID and regulation control for an autonomous mini-helicopter. *Information Sciences, 10*(177), 1999–2022.
3. Boukadida, W., Benamor, A., Messaoud, H., & Siarry, P. (2019). Multi-objective design of optimal higher order sliding mode control for robust tracking of 2-DoF helicopter system based on meta-heuristics. *Aerospace Science and Technology, 91*, 442–455.
4. Prempain, E., & Postlethwaite, I. (2005). Static H_∞ loop shaping control of a fly-by-wire helicopter. *Automatica, 9*(41), 1517–1528.
5. Zhang, Y., Wang, Q., Dong, C., & Jiang, Y. (2013). H_∞ output tracking control for flight control systems with time-varying delay. *Chinese Journal of Aeronautics, 5*(26), 1251–1258.
6. Li, R., Wu, Q., & Chen, M. (2017). Robust adaptive control for unmanned helicopter with stochastic disturbance. *Procedia Computer Science, 105*, 209–214.
7. Nicol, C., Macnab, C. J. B., & Ramirez-serrano, A. (2011). Robust adaptive control of a quadrotor helicopter. *Mechatronics, 6*(21), 927–938.
8. Yang, H., Jiang, B., Yang, H., & Liu, H. T. (2018). Synchronization of multiple 3-DOF helicopters under actuator faults and saturations with prescribed performance. *ISA Transactions, 75*, 118–126.
9. Chen, Y., Yang, X., & Zheng, X. (2018). Adaptive neural control of a 3-DOF helicopter with unknown time delay. *Neurocomputing, 307*, 98–105.
10. Yang, J., & Hsu, W. (2009). Adaptive backstepping control for electrically driven unmanned helicopter. *Control Engineering Practice, 8*(17), 903–913.
11. Sadala, S., & Patre, B. (2018). A new continuous sliding mode control approach with actuator saturation for control of 2-DOF helicopter system. *ISA Transactions, 74*, 165–174.
12. Wang, B., Yu, X., Mu, L., & Zhang, Y. (2019). Disturbance observer-based adaptive fault-tolerant control for a quadrotor helicopter subject to parametric uncertainties and external disturbances. *Mechanical Systems and Signal Processing, 120*, 727–734.
13. Asl, S., & Moosapour, S. (2017). Adaptive backstepping fast terminal sliding mode controller design for ducted fan engine of thrust-vectored aircraft. *Aerospace Science and Technology, 71*, 521–529.
14. Fang, X., & Shang, Y. (2019). Trajectory tracking control for small-scale unmanned helicopters with mismatched disturbances based

on a continuous sliding mode approach. *International Journal of Robust and Nonlinear Control, 1*, 1–15.

15. Fang, X., Wu, A., & Shang, Y. (2016). Robust control of small-scale unmanned helicopter with matched and mismatched disturbances. *Journal of the Franklin Institute, 53*(13), 4803–4820.

16. Koo, T., & Sastry, S. (1998). Output tracking control design of a helicopter model based on approximate linearization. In *Proceedings of the 37th IEEE conference on decision and control*, Tampa, FL, USA (Vol. 4, pp. 3635–3640).

17. Koo, T., & Sastry, S. (1999). Differential flatness based full authority helicopter control design. In *Proceedings of the 38th IEEE conference on decision and control*, Phoenix, AZ, USA (Vol. 2, pp. 1982–1987).

18. Liu, W., & Shi, P. (2019). Optimal linear filtering for networked control systems with time-correlated fading channels. *Automatica, 101*, 345–353.

19. Kanellakopoulos, I., Kokotovic, P., & Morse, A. (1991). Systematic design of adaptive controllers for feedback linearizable systems. *IEEE Transactions on Automatic Control, 11*(36), 1241–1253.

20. Frazzoli, E., Dahleh, M., & Feron, E. (2020). Trajectory tracking control design for autonomous helicopters using a backstepping algorithm. *Automatica, 6*, 4102–4107.

21. Lee, C., & Tsat, C. (2007). Improvement in trajectory tracking control of a small scale helicopter via backstepping. In *IEEE International Conference on Mechatronics*, Kumamoto, Japan (pp. 212–217)

22. Lungu, M. (2020). Auto-landing of UAVs with variable centre of mass using the backstepping and dynamic inversion control. *Aerospace Science and Technology, 103*, 105912.

23. Wang, J., Wang, C., Wei, Y., & Zhang, C. (2020). Filter-backstepping based neural adaptive formation control of leader-following multiple AUVs in three dimensional space. *Applied Ocean Research, 94*, 101971.

24. Wang, R., & Liu, J. (2018). Trajectory tracking control of a 6-DOF quadrotor UAV with input saturation via backstepping. *Journal of the Franklin Institute, 355*(7), 3288–3309.

25. Lungu, M. (2019). Auto-landing of fixed wing unmanned aerial vehicles using the backstepping control. *ISA Transactions, 95*, 194–210.

26. Yong, K., Chen, M., Shi, Y., & Wu, Q. (2020). Flexible performance-based robust control for a class of nonlinear systems with input saturation. *Automatica, 122*, 109268.

27. Yong, K., Chen, M., Shi, Y., & Wu, Q. (2021). Hybrid estimation strategy-based anti-disturbance control for nonlinear systems. *IEEE Transactions on Automatic Control, 66*(10), 4910–4917.

28. Zhao, Z., Yang, J., & Li, S. (2019). Composite nonlinear bilateral control for teleoperation systems with external disturbances. *IEEE/CAA Journal of Automatica Sinica, 6*(5), 1220–1229.

29. Yang, J., Liu, C., Coombes, M., et al. (2021). Optimal path following for small fixed-wing UAVs under wind disturbances. *IEEE Transactions on Control Systems Technology, 29*(3), 996–1008.

30. Yang, J., Zolotas, A., Chen, H., & Li, S. (2011). Robust control of nonlinear MAGLEV suspension system with mismatched uncertainties via DOBC approach. *ISA Transactions, 3*(50), 389–396.

31. Zhou, L., Cheng, L., She, J., & Zhang, Z. (2019). Generalized extended state observer-based reprtitive control for systems with mismatched disturbances. *International Journal of Robust and Nonlinear Control, 29*, 3777–3792.

32. Liu, C., Chen, W., & John, A. (2012). Tracking control of small-scale helicopters using explicit nonlinear MPC augmented with disturbance observers. *Control Engineering Practice, 20*, 258–268.

33. Ullah, I., & Pei, H. (2020). Fixed time disturbance observer based sliding mode control for a miniature unmanned helicopter hover operations in presence of external disturbances. *IEEE Access, 8*, 73173–73181.

34. Fang, X., Liu, F., & Zhao, S. (2019). Trajectory tracking control for manned submersible system with disturbances via disturbance characterization index approach. *International Journal of Robust and Nonlinear Control, 29*, 5641–5653.

35. Li, Y., Chen, M., Li, T., & Wang, H. (2020). Tracking control for the helicopter with time-varying disturbance and input stochastic perturbation. *ASCE Journal of Aerospace Engineering, 3*(24), 961–976.

36. Hao, S., Sun, Q., Wu, W., Chen, Z., & Tao, J. (2020). Altitude control for flexible wing unmanned aerial vehicle based on active disturbance rejection control and feedforward compensation. *International Journal of Robust and Nonlinear Control, 30*, 222–245.

37. Qian, W., Gao, Y., & Yang, Y. (2019). Global consensus of multiagent systems with internal delays and communication delays. *IEEE Transactions on Systems, Man, and Cybernetics: Systems, 49*(10), 1961–1970.

38. Qian, W., Xing, W., & Fei, S. (2021). H_∞ state estimation for neural networks with general activation function and mixed time-varying delays. *IEEE Transactions on Neural Networks and Learning Systems, 32*(9), 3909–3918.

Linbo Chen received his B.Sc. degree in engineering from Civil Aviation Flight University of China in 2019, and currently, he is an M.Sc. degree candidate at School of Automation Engineering of Nanjing University of Aeronautics and Astronautics, China. His research includes anti-disturbance control with its application to flight control system.
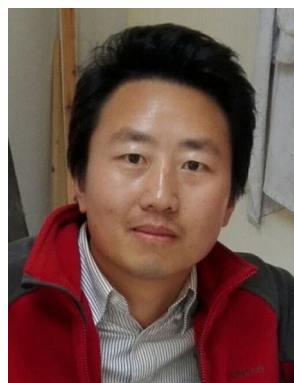
Tao Li received his Ph.D. degree in engineering from Southeast University in 2008 and was a postdoctoral research fellow at School of Instrument Science and Engineering of Southeast University during year 2008 and 2011, China. He has been a visiting scholar at Control System Center of The Manchester University from year 2016 to 2017, UK. He is currently a professor at the School of Automation Engineering, Nanjing University of Aeronautics and Astronautics in China. His current research interests include neural networks, time-delay systems, networked control systems, and unmanned aerial helicopter.
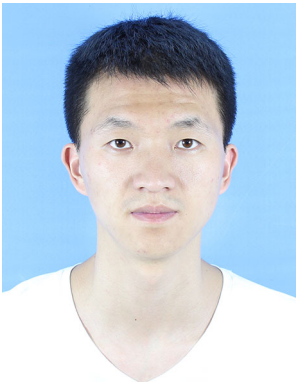
Lijun Liu received his M.Sc. degree at the College of Mathematics and Information Science, Guangxi University, Nanning, in 2017. He is currently pursuing a Ph.D. degree in control theory and control engineering from the College of Automation Engineering, Nanjing University of Aeronautics and Astronautics, Nanjing. His current research interests include nonlinear system control and flight control.

Zehui Mao received the Ph.D. degree in control theory and control engineering from the Nanjing University of Aeronautics and Astronautics, Nanjing, China, in 2009. She was a visiting scholar with the University of Virginia from 2015 to 2016. She worked in the fields of fault diagnosis, with particular interests in nonlinear control systems, sampled-data systems, and networked control systems. She is currently a professor with the College of Automation Engineering, Nanjing University of Aeronautics and Astronautics. Her current research interests include fault diagnosis and fault-tolerant control of systems with disturbance and incipient faults and high-speed train and spacecraft flight control applications.